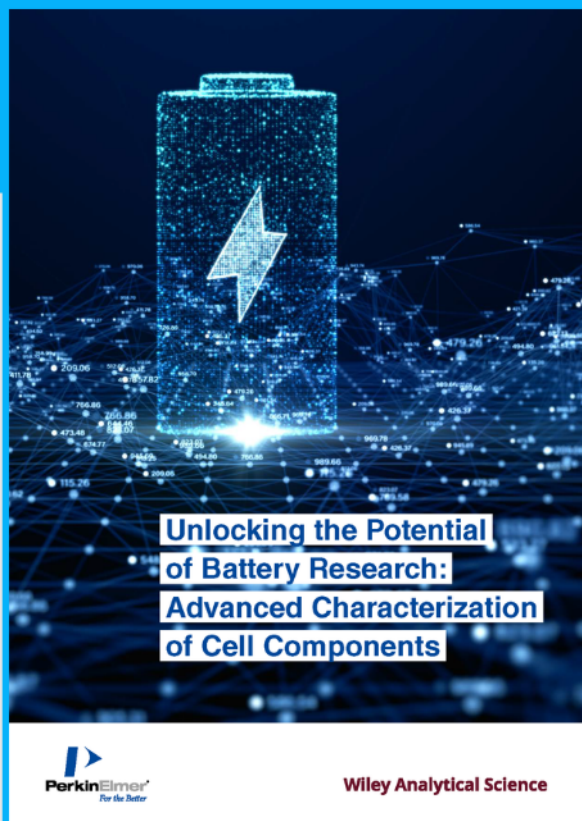




Unlocking the Potential of Battery Research



**A New Expert Insight.
Download for free.**

Battery research is essential to meet the growing demand for reliable, efficient, cost-effective energy storage solutions.

This expert insight presents recent research on solid polymer electrolytes (SPEs), recycling methods for lithium-ion batteries (LIBs), and cathode degradation during extreme fast charging (XFC) of electric vehicles.



Design and simulation of a UOIT copper–chlorine cycle for hydrogen production

Mehmet F. Orhan^{1,*}, Ibrahim Dincer² and Marc A. Rosen²

¹Department of Mechanical Engineering, College of Engineering, American University of Sharjah, PO Box 26666, Sharjah, United Arab Emirates

²Faculty of Engineering and Applied Science, University of Ontario Institute of Technology, 2000 Simcoe Street North, Oshawa, Ontario, L1H 7 K4, Canada

SUMMARY

A design and simulation study of the four-step copper–chlorine (Cu–Cl) cycle using Aspen Plus software (Aspen Technology Inc., Cambridge, MA) is reported. The simulation consists of four main sections: hydrolysis, oxy-decomposition, electrolysis, and drying. This paper explains and justifies how the actual reaction kinetics is factored into these four main sections. Also, it illustrates all the process units that are used in the simulation of four-step Cu–Cl cycle, providing their associated specifications and design parameters. It is found that hydrolysis reactors with smaller capacities and larger ($\geq 10/1$) steam to CuCl ratios were desirable to increase the reaction efficiency and prevent the formation of side products such as CuO and CuC. In contrast, larger capacity oxy-decomposition reactors with longer residence times are preferable to allow enough time for the copper oxychloride to decompose. Therefore, 10 (or more) small-scale hydrolysis reactors can feed one oxy-decomposition reactor with large capacity to keep continuity of the flow in the overall cycle. On the basis of the process flow sheet, a pinch analysis is developed for an integrated heat exchange network to enable effective heat recovery within the Cu–Cl cycle. Copyright © 2012 John Wiley & Sons, Ltd.

KEY WORDS

hydrogen production; thermochemical water decomposition; nuclear; copper–chlorine cycle; simulation; design; Aspen Plus

Correspondence

*Mehmet F. Orhan, Department of Mechanical Engineering, College of Engineering, American University of Sharjah, PO Box 26666, Sharjah, United Arab Emirates.

†E-mail: morhan@aus.edu

Received 31 January 2012; Revised 2 April 2012; Accepted 4 April 2012

1. INTRODUCTION

In today's world, energy and its transformation play critical roles in our lives and have a direct impact on every sector of society, affecting the overall economic and societal well-being. Generally, economic and human health are linked to per capita energy consumption. Energy is used in almost every human activity, including transportation, household uses, agriculture, industry and manufacturing, and buildings. Energy is consumed both directly in some uses and indirectly in others through use of materials that require energy in their production or delivery.

Hydrogen is expected to play a significant role as an energy carrier, and demand for it is expected to increase in the near future, for it can be utilized as clean fuel in diverse energy end-use sectors including conversion to electricity with no direct CO₂ emission. Hydrogen can also be stored and transported over long distances with lower losses compared with electricity. But hydrogen is not an energy source as it does not exist in abundance naturally

in its elemental form. Therefore, hydrogen has to be produced, and this is normally carried out from fossil fuels and/or water.

Thermochemical water splitting with a copper–chlorine (Cu–Cl) cycle is a promising process to decompose water into its constituents, oxygen and hydrogen, through intermediate copper and chlorine compounds. These chemical reactions form a closed internal loop that recycles all chemicals on a continuous basis, without emitting any greenhouse gases. Thermochemical water splitting with a Cu–Cl cycle is a promising process that could be linked with nuclear reactors or solar thermal energy.

The Cu–Cl cycle has not yet been proven or constructed. However, many studies of the Cu–Cl cycle have been reported. For example, Al-Dabbagh and Lu [1] have studied the design and reliability of control systems for a Cu–Cl thermochemical hydrogen production plant. Equilibrium conversion in the Cu–Cl cycle multiphase processes has been studied by Daggupati *et al.* [2]. They performed a thermodynamic equilibrium analysis of individual

steps in the cycle. Recently, they studied solid particle decomposition and hydrolysis reaction kinetics in Cu–Cl [3] and a solid conversion process during hydrolysis and decomposition of cupric chloride in the Cu–Cl cycle [4].

One of the most challenging steps in the thermochemical Cu–Cl cycle is the hydrolysis of CuCl_2 into Cu_2OCl_2 and HCl while avoiding the need for excess water and the undesired thermolysis reaction, which yields CuCl and Cl_2 . Argonne National Laboratory has designed a spray reactor where an aqueous solution of CuCl_2 is atomized into a heated zone, into which steam/Ar are injected in co-current or counter-current flow [5]. Also, an experimental study using a spray reactor with an ultrasonic atomizer has been carried out [6].

Jaber *et al.* [7] have studied heat recovery from molten CuCl in the Cu–Cl cycle. They examined the convective heat transfer between molten CuCl droplets and air in a counter-current spray flow heat exchanger.

Ceramic carbon electrode-based anodes for use in the Cu–Cl cycle have been studied by Ranganathan and Easton [8,9]. Ceramic carbon electrode materials, prepared using 3-aminopropyl trimethoxysilane, are investigated in their study.

Wang *et al.* [10] have compared sulfur–iodine and Cu–Cl thermochemical hydrogen production cycles from the perspectives of heat quantity, heat grade, thermal efficiency, related engineering challenges, and hydrogen production cost.

Thermophysical properties of copper compounds in the Cu–Cl cycle have been studied by Zamfirescu *et al.* [11]. Also, the kinetics has been studied of the copper/hydrochloric acid reaction in the Cu–Cl [12].

Issues related to equipment scale-up and process simulation were examined by Rosen *et al.* [13]. The study basically outlines the challenges and the design issues of hydrogen production with the Cu–Cl cycle. The system was simulated using Aspen Plus to find efficiencies. The total heat requirement to produce 1 mole of hydrogen using the Cu–Cl cycle was calculated as 543.7 kJ, and the energy efficiency was found to be about 53% [13].

Naterer *et al.* [14] reported recent Canadian advances in nuclear-based hydrogen production and the thermochemical Cu–Cl cycle, including aspects of individual process and reactor developments within the Cu–Cl cycle, thermochemical properties, advanced materials, controls, safety, reliability, economic analysis of electrolysis at off-peak hours, and integration of hydrogen plants with Canada's nuclear plants.

Design issues associated with reactor scale-up in the thermochemical Cu–Cl cycle have been examined by Wang *et al.* [15]. The study focused on hydrolysis, hydrogen, and oxygen reactors. Scale-up design issues with molten salt reactor for handling of three phase material, including copper solid oxychloride particles, molten salt, and oxygen have been studied. Moreover, variations of hydrolysis reactor for the two-step, three-step, and five step Cu–Cl cycles have been analyzed.

Lewis *et al.* [16,17] have reported that the Cu–Cl cycle is chemically viable with respect to engineering and energy efficiency. A conceptual process incorporating Aspen Plus

mass and energy flows were designed, and the hydrogen production cost was estimated as \$3.30 per kg hydrogen.

The main objectives of this paper are to design and simulate the four-step Cu–Cl cycle using Aspen Plus process simulation software. With the use of the simulation, main steps of the Cu–Cl cycle are evaluated individually to determine how each process reacts to varying key operating and design variables. A sensitivity analysis is performed by varying one or more flow sheet variables to study the effect of that variation on other variables to achieve a simple process optimization. This paper also explains how the actual reaction kinetics is factored into the main steps of the Cu–Cl cycle. Process units used in the simulation of four-step Cu–Cl cycle are illustrated, providing all their associated specifications and design parameters. On the basis of the flow sheet, a pinch analysis is developed for an integrated heat exchange network to enable effective heat recovery within the Cu–Cl cycle. Finally, a comparison of design and operation conditions of individual components in the cycle is made on the basis of a small scale experimental work on individual reactions in the cycle, conducted at the Clean Energy Research Laboratory (CERL) at the University of Ontario Institute of Technology (UOIT) in Oshawa, Canada.

2. SYSTEM STUDIED

An overview is presented of research activities on the Cu–Cl cycle in the CERL at UOIT. This experimental setup is one of the world's first lab-scale demonstrations of the Cu–Cl cycle of thermochemical water splitting for nuclear hydrogen production (see [18] for further details). The setup is based on the four-step Cu–Cl cycle described in Figure 1.

The hydrogen production step (Step 1 in Figure 1) is a major reaction step taking place in the electrolyzer to produce hydrogen. The electrochemical reaction between cuprous chloride (CuCl) and hydrochloric acid (HCl) produces hydrogen gas and cupric chloride. The cupric chloride generated from this step is used for regenerating CuCl and HCl, using water and heat for continuous production of hydrogen. The electrolysis reactor, the hydrogen production step, has not been built in the CERL yet. However, experiments on this step are being carried out by Atomic Energy of Canada Limited, a project partner, demonstrating that hydrogen can be produced at a current density of 0.1 A/cm^2 for a cell voltage in the range of 0.6–0.7 V. A schematic of the experimental layout is illustrated in Figure 2.

The drying step (Step 2 in Figure 1) utilizes low-grade heat to generate cupric chloride powder from the effluent cupric chloride solution mixture exiting from the electrolysis step, Step 1. Figure 3 shows the experimental spray dryer unit at the CERL.

In the hydrolysis step (Step 3 in Figure 1), solid cupric chloride generated from the previous step, Step 2, is contacted with steam at high temperatures around 400°C to split water, and form copper oxychloride and hydrogen chloride. The hydrogen chloride is recycled back to Step 1, and the solid cupric chloride moves to Step 4 for oxygen

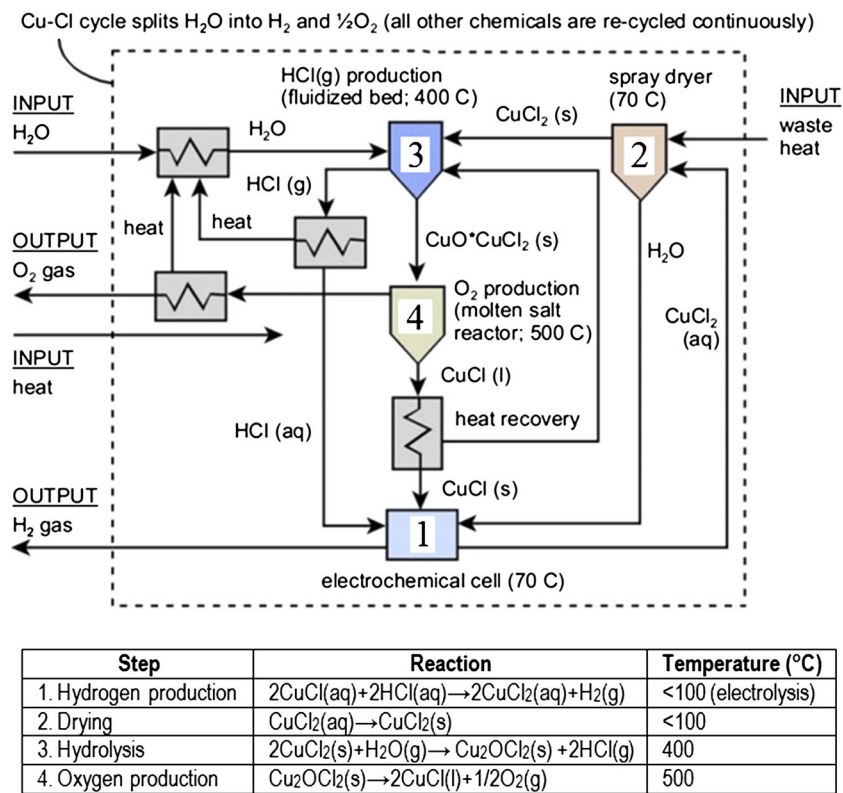


Figure 1. Schematic of process flow diagram for the Cu–Cl cycle in the Clean Energy Research Laboratory (adapted from [14]).

production. Figures 4 and 5 show the experimental units in the CERL for the hydrolysis reaction.

In Figure 4, the cold-model fluidized-bed unit in the experiment has an internal fluidized column diameter of 0.1 m. It is made of Perspex glass. Copper, glass solids, and air can be used for the experiment. Three pressure taps

(2 differential, 1 absolute) are located for both differential and absolute dynamic pressure measurements. Various aspect ratios, particle sizes, and distributor plate geometries can be used for the experiments.

The fluidized-bed unit also includes a downstream-processing network. The main purpose of the downstream-

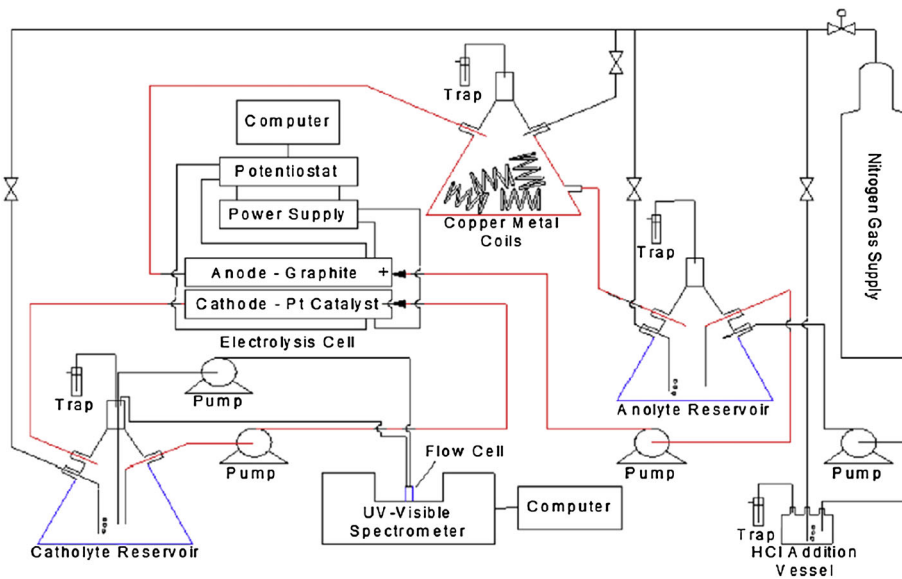


Figure 2. Single cell process flow diagram [20].



Figure 3. Experimental spray dryer unit with scrubber.

processing network in the pilot size Cu–Cl cycle is to cool, condense, and neutralize the CuCl laced steam. In the closed loop cycle, which will be employed for the industrial-sized cycle, there will be no need for a downstream network as all chemicals will be recycled within the cycle. However, because of the semi-continuous operation of the pilot scale setup in the CERL, it is required that the steam be neutralized after exiting the hydrolysis reactor.

The downstream network consists of three main sections: heat exchanger, separator, and scrubbing sections. Glycol and a CuCl laced steam enter the heat exchanger section, and the steam is cooled and condensed before entering the separator. The separator is used to separate two phases of the flow. The fluid is extracted and neutralized. Non-condensable

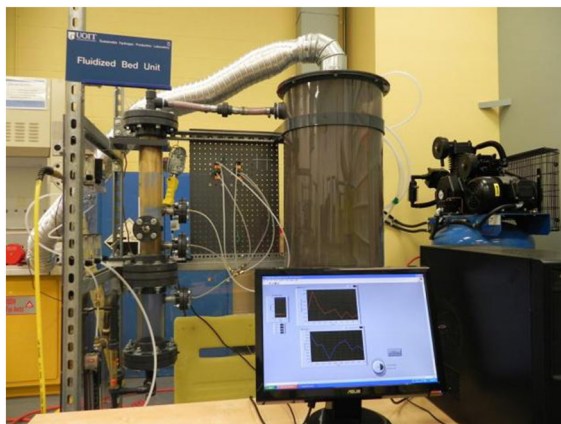


Figure 4. Low-temperature fluidized-bed reactor for the hydrolysis reaction.



Figure 5. Experimental hydrolysis reactor with accessories, steam boiler, and superheater.

gases are then blown to a packed bed scrubber to be cleaned and exhausted to the atmosphere.

In oxygen production step (Step 4 in Figure 1), copper oxychloride produced from the hydrolysis step is decomposed to produce cuprous chloride (CuCl) and oxygen gas. The CuCl is recycled back to the electrolysis step for hydrogen production, and the oxygen is a byproduct. Figure 6 shows the experimental setup of the oxygen production reactor in the CERL.

3. EFFICIENCY ANALYSIS

Energy supply in the past decades, at present, and in the future is the outcome of market coverage, and it is determined by main players of a very different kind such as supply sources and efficiency. Efficiency is crucial for the structure of the demand for energy. Energy demand of thermodynamic systems can be reduced very significantly by increasing their efficiency. Thus, efficiency has received wider acceptance and is now seen as an important tool for sustainable development.



Figure 6. High-temperature experimental unit for copper oxychloride decomposition and oxygen production.

The heat transfer for a chemical process involving no work interaction W is determined from the energy balance $\dot{E}_{in} - \dot{E}_{out} = \Delta \dot{E}_{system}$ applied to a system with $W=0$. For a steady-state reaction process, the energy balance reduces to

$$\bar{Q} = H_p - H_R = \sum n_P (\bar{h}_f^\circ + \bar{h} - \bar{h}^\circ)_P - \sum n_R (\bar{h}_f^\circ + \bar{h} - \bar{h}^\circ)_R \quad (1)$$

The overall energy efficiency of the Cu–Cl cycle, η_e , can be described as the fraction of energy supplied that is converted to the energy content of H_2 on the basis of its lower heating value:

$$\eta_e = \frac{\bar{E}_{out}}{\bar{E}_{in}} = \frac{\overline{LHV}_{H_2}}{(\bar{Q}_{net} + \bar{W})_{in}} \quad (2)$$

where \overline{LHV}_{H_2} is the lower heating value of hydrogen, \bar{W} is the electrical work required for the electrolyzer and auxiliary work required for pumps, compressors, and so on, and \bar{Q}_{net} is the net heat (after subtracting the recovered heat) used by the process to produce a unit amount of product hydrogen, all per mole of hydrogen produced. Therefore, Equation (2) can be rewritten as the following to evaluate the effect of the effectiveness of the heat exchangers (ε) on the overall efficiency of the cycle (η_e),

$$\eta_e = \frac{\overline{LHV}_{H_2}}{\left(\frac{\bar{Q}_{required}}{\varepsilon} - \varepsilon \bar{Q}_{recovered} \right) + \bar{W}} \quad (3)$$

The lower heating value of hydrogen is 240 kJ/mol H_2 . The overall exergy efficiency of the Cu–Cl cycle is expressed as

$$\eta_{ex} = \frac{e\bar{x}_{out}}{e\bar{x}_{in}} \quad (4)$$

where $e\bar{x}_{out}$ and $e\bar{x}_{in}$ are output and input molar exergies. Using the exergy balance in Equation (4) for the Cu–Cl cycle, the exergy efficiency can be written alternatively as

$$\eta_{ex} = \frac{e\bar{x}_{H_2}}{\bar{W} + \sum_i \left(1 - \frac{T_0}{T_i} \right) \bar{Q}_i} \quad (5)$$

where $e\bar{x}_{H_2}$ is the exergy content of the hydrogen produced, which is taken as 236.12 kJ/mol in this paper. For the overall cycle, we obtained the total input exergy of the cycle by adding the total work requirement and exergy content of net heat input to the cycle. Again, in the summation of input exergy, the exothermic reaction (i.e., the hydrogen production reaction of five-step Cu–Cl cycle) is taken as negative, assuming this energy can be used for other endothermic reactions.

4. PROCESS DESIGN OF THE Cu–Cl CYCLE

Based on the extensive literature review carried out, no (or little) previous work has been performed on the realistic modeling of the electrolyzer in the Cu–Cl cycle. In the prior simulations, a simple stoichiometric reactor model has been used for the electrolyzer. Because there was insufficient data to model the electrolyzer, the inlet and outlet compositions have been defined for the cathode and anode streams, and values for the cell voltage and current density have been assumed. This study presents an Aspen Plus simulation that includes a realistic model of the electrolyzer written as a user-defined Fortran model. The Aspen Plus model is developed in three steps. At first, a flow sheet is developed in which all reactors are stoichiometric with reactions going to completion. Secondly, equilibrium reactors (i.e., REquil and RGibbs) are used for more realistic approach to process reactions. The chemical reactions are assumed to achieve thermodynamic equilibrium under the specified flow rates and operating conditions. The HeatX module of Aspen Plus is used to model the heat exchangers. The final step involves the inclusion of the Fortran code to describe the operation of the electrolyzer.

While developing a flow sheet of the Cu–Cl cycles, at first, the thermodynamic database used in the Aspen Plus simulation is updated. For example, to prepare a more realistic simulation, values of the enthalpy of formation, the free energy of formation, and the heat capacity as a function of temperature for Cu_2OCl_2 had to be defined. Because Cu_2OCl_2 is not commercially available, a new experimental method for synthesizing it was developed by Lewis *et al.* [16,17]. The enthalpy of formation at 25 °C was measured using two different methods and compared with the literature data. A value of 380 ± 3 kJ/mol was determined to be the most reliable. The heat capacity was measured over three temperature regions: (i) from about 4 (liquid He temperature) to 64 K (liquid N_2 temperature); (ii) from 64 to 360 K; and (iii) from 298 to 700 K. The low-temperature heat capacities were used to calculate the entropy. The free energy of formation was then derived from the experimental values for the enthalpy of formation and entropy values. Also, CuCl undergoes a solid–solid transition and then a solid–liquid transition. The specific enthalpy and Gibbs energy of formation of CuCl(s) at the standard temperature of 298.15 K are -37.0 kJ/mol and -120.0 kJ/mol, respectively. The Gibbs energy of formation of CuCl(s) was obtained by subtracting the product of the entropy of formation of CuCl at 298.15 K and the absolute temperature, 298.15 K, from the enthalpy of formation of CuCl at 298.15 K.

In this study, all thermodynamic data for the various chemical species is defined from literature and included in the physical property database of Aspen Plus (see Table I). In addition, the reliability of the data for the other compounds is also checked by comparing data in various sources such as HSC Chemistry software.

In the literature, five-step [19], four-step [14,20], and three-step [16,17] configurations of the Cu–Cl cycle have

Table I. Thermodynamic data used in the Aspen Plus Database.

Compound	DHSFRM (kJ/mol)	DGSFRM (kJ/mol)
CuCl ₂ (s)	−217.4	−173.6
CuO (s)	−162.0	−129.4
CuCl (s)	−137.0	−120.0
Cu (s)	0	0
Cu ₂ OCl ₂ (s)	−381.3	−310.45

DHSFRM: Enthalpy of formation at 298.15 K and 1 bar.
 DGSFRM: Gibbs free energy of formation at 298.15 K and 1 bar.
 Source: [22].

been presented. Some of these configurations have remained only as some ideas in theoretical studies. In contrast, an experimental setup is being prepared for the four-step Cu–Cl cycle at UOIT and three-step Cu–Cl cycle at the Argonne National Lab in the US. This study focus on the four-step Cu–Cl cycle so that the simulation results in this study can be compared with the experimental results at UOIT.

The overall process flow sheet of the four-step Cu–Cl cycle is shown in Figure 7, for which Aspen Plus was used to develop mass and energy balances for a process based

on four main reactions (see Figure 1). In Figure 7, heat exchangers are denoted by HE (see [21] for detailed analysis of heat exchangers in the Cu–Cl cycle). Also, H and C represent hot and cold streams, respectively. For example, HE1-H denotes the hot stream of heat exchanger 1 and HE1-C the cold stream of heat exchanger 1. The *HeatX* option of Aspen Plus is used to simulate heat exchange between two (hot and cold) streams. Equilibrium-based reactors are used to simulate chemical reactions. *REquil* and *RGibbs* options are used to simulate hydrolysis and oxy-decomposition, respectively. Also, a user-defined reactor model is used for electrolysis, and the *Flash2* separator model of Aspen Plus is used for the drying process.

On the basis of the flow sheet in Figure 7, a pinch analysis is developed for an integrated heat exchange network to enable effective heat recovery within the Cu–Cl cycle. The heat exchanger network is presented in Figure 8, and its specifications are presented in Table II. The heat exchanger parameter values in Figures 7 and 8 are identical.

Tables III and IV describe all the process units that are used in the simulation of the four-step Cu–Cl cycle in Figure 7, providing their associated specifications and design parameters.

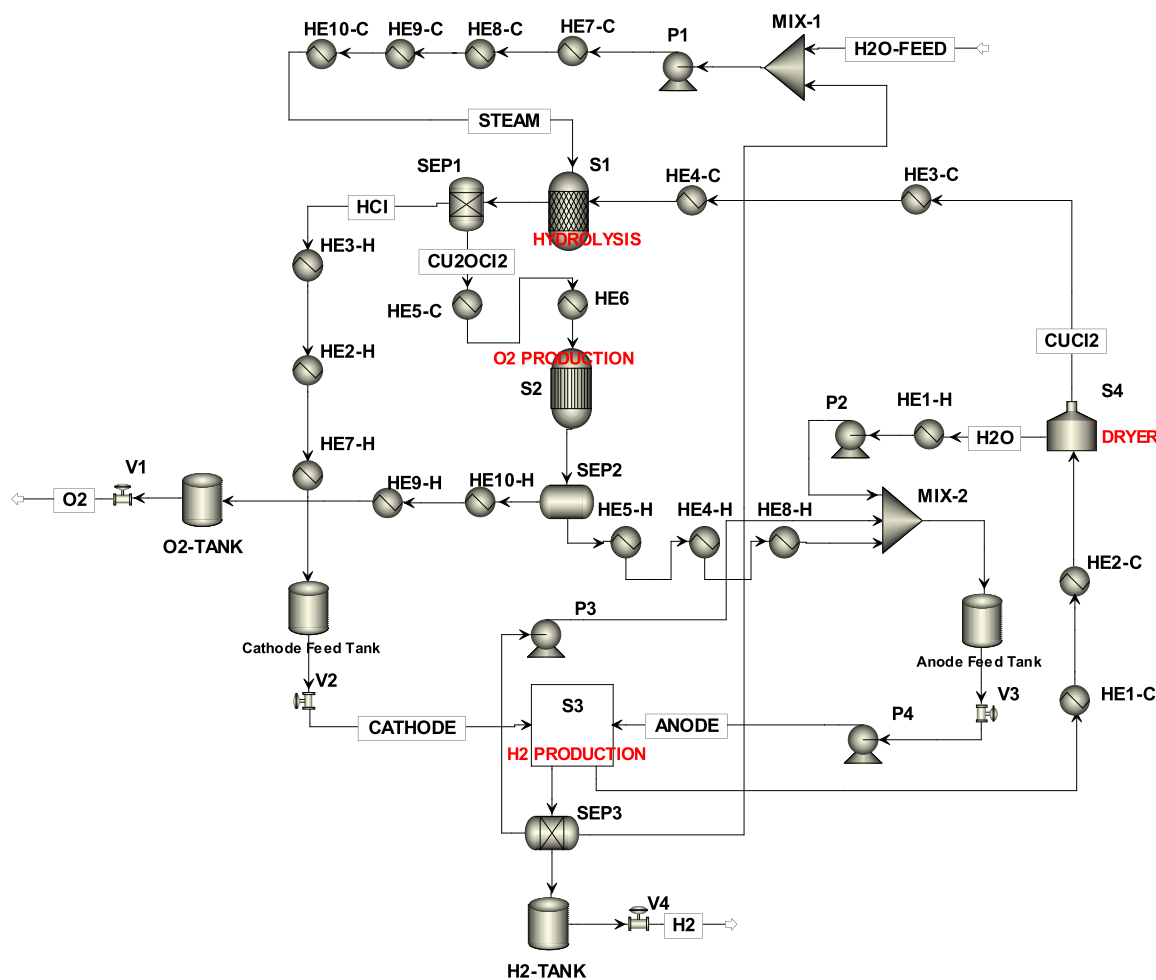


Figure 7. Simplified Aspen Plus flow sheet of the four-step Cu–Cl cycle.

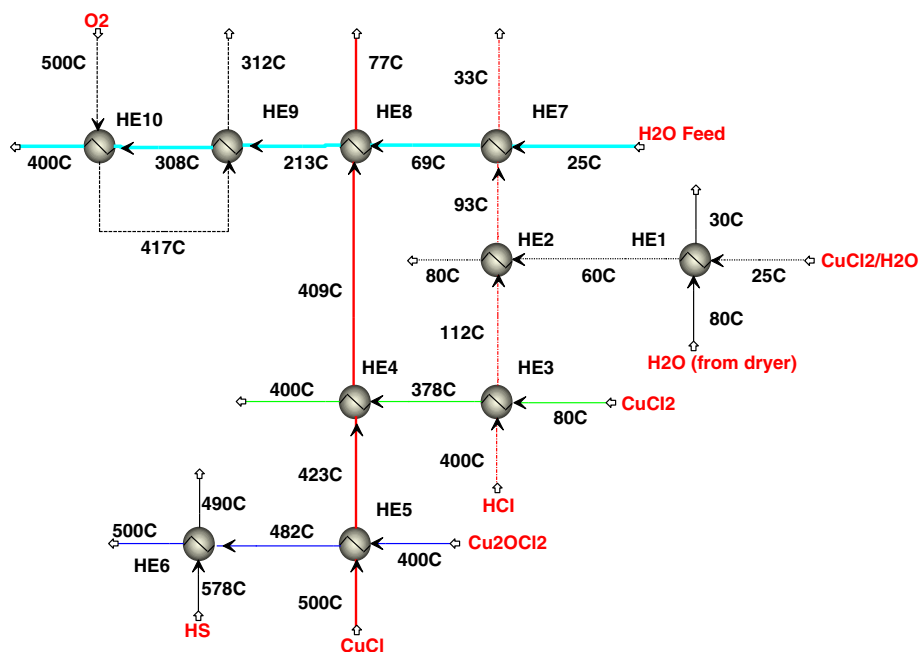


Figure 8. Aspen Plus flow sheet of heat exchanger network (HS: Heat source).

The simulation in Figure 7 consists of four main sections: hydrolysis, oxy-decomposition, electrolysis, and drying. Figures 9–13 explain and justify how the actual reaction kinetics is factored into these four main sections. Hydrolysis is Step 1 of the Cu–Cl cycle and is denoted S1 in Figure 7. In the hydrolysis reactor, the hot and pressurized CuCl_2 is sprayed into a superheated vapor environment at 400°C , forming a free jet. Thermal energy is used to preheat the streams (see Figure 9). Spraying process takes place at 24 bar so that it forms a free jet. This high pressure is used to expand the CuCl_2 and aspirates the superheated steam into the jet. As the jet expands, it aspirates the superheated steam into the jet resulting in high mass and heat transfer between the CuCl_2 in the jet and the steam. The CuCl_2 is then converted to Cu_2OCl_2 and HCl . The chemical reaction

equation is $2\text{CuCl}_2(\text{s}) + \text{H}_2\text{O}(\text{g}) \rightarrow \text{CuO} \cdot \text{CuCl}_2(\text{s}) + 2\text{HCl}(\text{g})$. The HCl and steam exit the hydrolysis reactor, and are cooled and fed to the cathode part of electrolysis section. Also, solid Cu_2OCl_2 accumulates at the bottom of the hydrolysis reactors because of gravitation. The solid Cu_2OCl_2 is then transferred to the oxy-decomposition reactor.

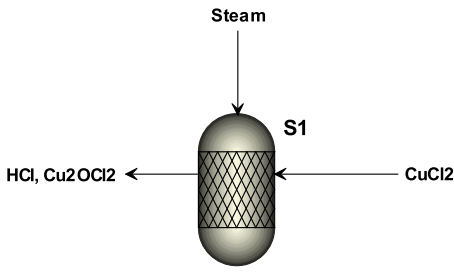
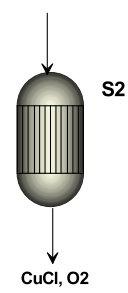
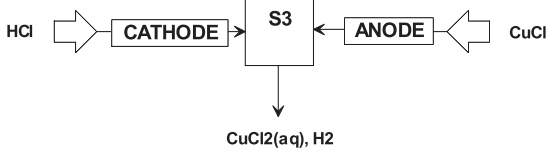
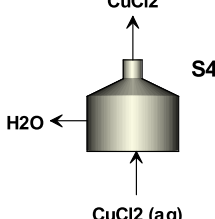
In the oxy-decomposition reactor (see Figure 10), the Cu_2OCl_2 is heated to 500°C using thermal energy. At 500°C , the Cu_2OCl_2 decomposes to O_2 and molten CuCl . The oxygen leaves at the top of oxy-decomposition reactor as a gas flow, and the CuCl spills over a weir to a separate section. CuCl is then pumped back to the anode feed tank.

Figure 11 demonstrates the electrolysis process in the four-step Cu–Cl cycle. The CuCl is added to the anode feed tank in aqua form. The dissolved CuCl is then

Table II. Specifications for heat exchangers in the four-step Cu–Cl cycle.

Heat exchanger	Hot stream				Cold stream		
	ID	Temperature ($^\circ\text{C}$)		ID	Temperature ($^\circ\text{C}$)		
		In	Out		In	Out	
HE1	HE1-H	80	30	HE1-C	25	60	
HE2	HE2-H	112	93	HE2-C	60	80	
HE3	HE3-H	400	112	HE3-C	80	378	
HE4	HE4-H	423	409	HE4-C	378	400	
HE5	HE5-H	500	423	HE5-C	400	482	
HE6	HS	578	490	HE6	482	500	
HE7	HE7-H	93	33	HE7-C	25	69	
HE8	HE8-H	409	77	HE8-C	69	213	
HE9	HE9-H	417	312	HE9-C	213	308	
HE10	HE10-H	500	417	HE10-C	308	400	

Table III. Reactor process units used in the simulation and their specifications.

Process unit	ID	Description (model)	Temp. (°C)	ΔH	
				(kJ/molH ₂)	W (kJ/molH ₂)
	S1	Hydrolysis (REquil)	400	120.2	-
	S2	Decomposition (RGibbs)	500	125.5	-
	S3	Electrolysis (User-defined)	25	-	55
	S4	Drying (Flash2)	80	-	33.2

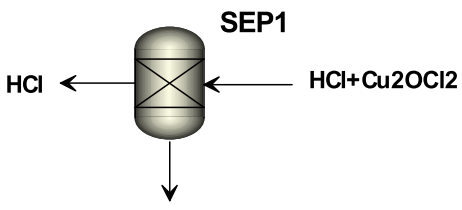
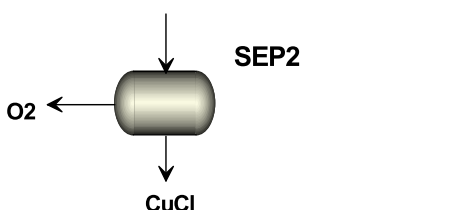
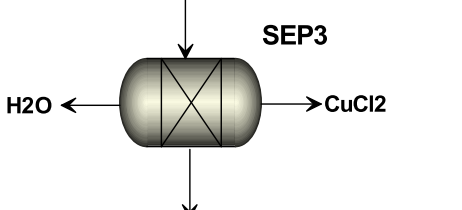
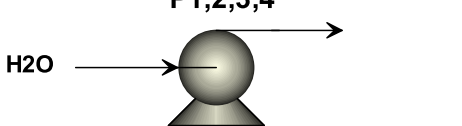


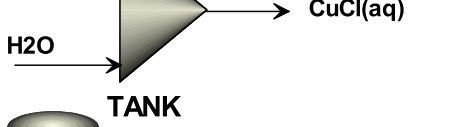

pumped to the anode section of the electrolyzer. Chloride ions migrate from the cathode across the electrolyzer membrane and react at the anode with the CuCl to form CuCl₂ (see Figure 12). The aqueous CuCl₂ is then transferred to the dryer (see Figure 13). Also, aqueous HCl is pumped from the cathode feed tank to the cathode, where the H⁺ ions are reduced to form H₂. The Cl⁻ ions transfer across the electrolyzer membrane as described previously. Water from the cathode is superheated to 400 °C and recycled to the hydrolysis section.

Simulation of the process flow sheet in Figure 7 provides stream flows and properties, heat duties as well as auxiliary work requirements for the four-step Cu–Cl cycle. For example, the mass flow rates of main streams are given in Table V. However, the results obtained from the simulation may vary on the basis of specified conditions and inputs to the simulation. After many runs of simulation at various reaction conditions, it is found that (in general) the hydrolysis reactors with

smaller capacities and larger (10/1 and more) steam to CuCl ratios are desirable to increase the reaction efficiency and prevent the formation of side products such as CuO and CuC. In contrast, larger capacity oxy-decomposition reactors with longer residence time are preferable to allow enough time for the copper oxychloride to decompose. Therefore, 10 (or more) small-scale hydrolysis reactors can feed one oxy-decomposition reactor with large capacity to keep continuity of the flow in the overall cycle.

The thermodynamic database was expanded to make it capable of handling the reactions to facilitate study of the hydrolysis reaction. The focus of the sensitivity analysis for the hydrolysis reactor is to maximize the yield of CuO*-CuCl₂ while minimizing the formation of side products. The results of these sensitivity studies are shown in Figures 14 and 15. The hydrolysis reactor is modeled with a feed of various water steam and CuCl₂ ratios (H₂O/CuCl₂). Figure 14 shows the effect of reaction temperature on the

Table IV. Auxiliary equipment models and their specifications.

Process unit	ID	Description (model)	Temp. (°C)	W (kJ/molH ₂)
	SEP1	Separator (Sep)	400	0.87
	SEP2	Separator (Sep)	500	1.2
	SEP3	Separator (Sep)	25	1
	P1,P2,P3,P4	Pump (Pump)	25	4.93
	MIX-1	Mixer (Mixer)	25	0.4
	MIX-2	Mixer (Mixer)	25	0.31
	O2-TANK H2-TANK	Storage Tank (TANK)	25	-
	V1, V2, V3, V4	Valve (Valve)	25	-

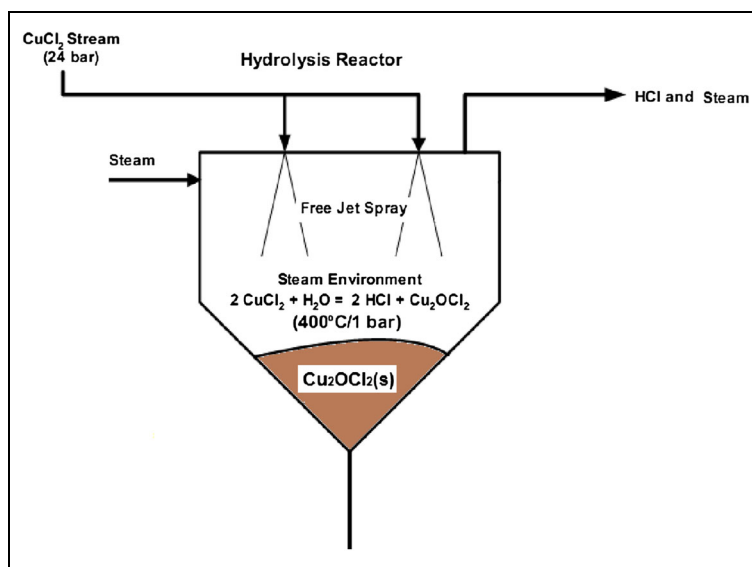


Figure 9. Hydrolysis reactor of the second option of the four-step Cu–Cl cycle (adapted from [22]).

$\text{CuO}^*\text{CuCl}_2$ yield at a $\text{H}_2\text{O}/\text{CuCl}_2$ ratio of 10, 15, and 20. As can be seen from the figure, the $\text{CuO}^*\text{CuCl}_2$ yield increases with reaction temperature up to 400 °C. Above that point, it starts decreasing. Also, an excess of steam is required for achieving high yields of $\text{CuO}^*\text{CuCl}_2$. For example, to achieve a yield of 70% (and more) mol of $\text{CuO}^*\text{CuCl}_2$ at 400 °C, an $\text{H}_2\text{O}/\text{CuCl}_2$ ratio of more than 10 is needed. The effect of $\text{H}_2\text{O}/\text{CuCl}_2$ ratio on the $\text{CuO}^*\text{CuCl}_2$ generation can be seen more clearly in Figure 15.

The results in Figure 15 are obtained at reaction temperatures of 350, 400, and 450 °C. The effect of $\text{H}_2\text{O}/\text{CuCl}_2$ ratio

on $\text{CuO}^*\text{CuCl}_2$ yield is significant until a ratio of 20. Above a feed ratio of 20, this effect starts to decrease, and it becomes constant at an $\text{H}_2\text{O}/\text{CuCl}_2$ ratio of 40 after $\text{CuO}^*\text{CuCl}_2$ yield reaches its peak value of 80% mol.

The results of the sensitivity analysis for the oxy-decomposition step are shown in Figure 16, in which the effect of reaction temperature on oxygen production is investigated. The results show that oxygen generation starts at a temperature as low as 350 °C and increases to a peak point at around 450 °C for reaction efficiency (η) values of both 100% (complete reaction) and 80%. The oxygen yield remains fairly constant with an increase in temperature above 450 °C. Traces of side products (i.e., chlorine gas) are also observed in this model analysis at incomplete reaction cases. The side-products generation increases with temperature and peaks at about 450 °C and then starts to decline as the temperature of the reactor is raised. At a reactor temperature of 550 °C, the generation rate of side products is negligible. Thus, undesirable side products can be eliminated by a better reactor design and optimization of operating conditions.

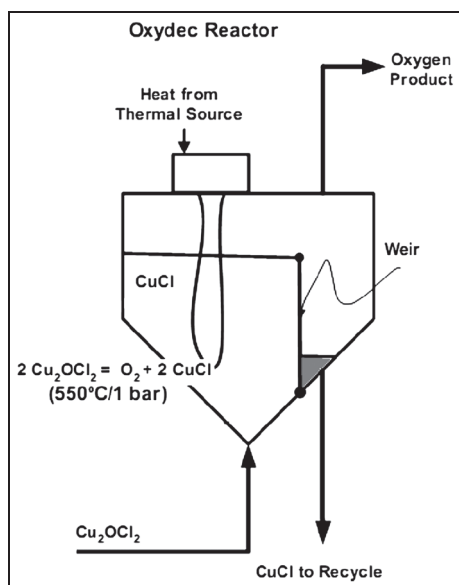


Figure 10. Oxy-decomposition reactor of the second option of the four-step Cu–Cl cycle (adapted from [22]).

5. VALIDATION

The Cu–Cl cycle has not yet been scaled up sufficiently to the level of industrial equipment, and it is still at the stage of proof-of-principle and small bench-scale apparatus. Thus, there are few previous studies on the same subject that the results of this study can be compared with. Nonetheless, to facilitate the validation of the simulation models, a comparison is made in three stages. First, the simulation is compared with the previous thermodynamic analyses to make sure that the results are within the boundary of thermodynamic laws and logic. Secondly, although the present experimental studies by the UOIT and other partners are at the level of small

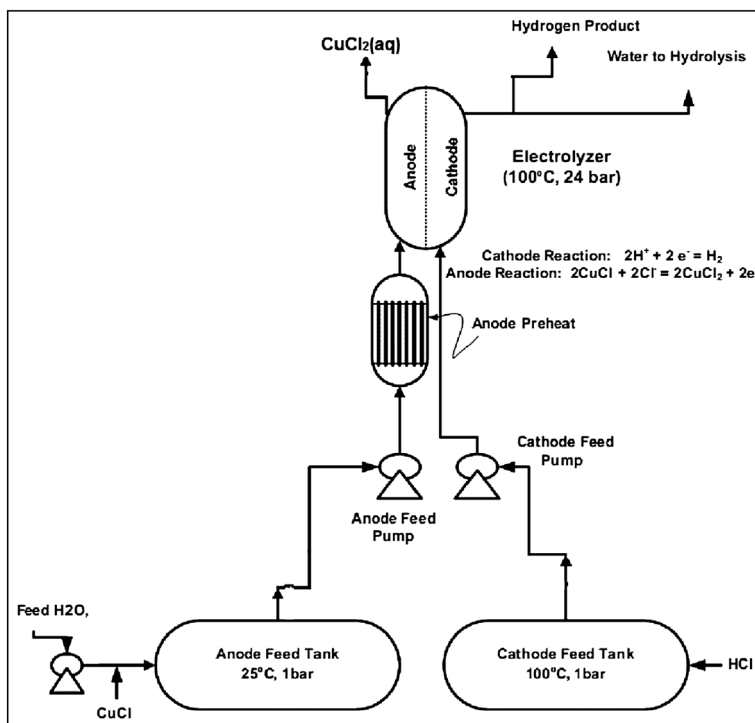


Figure 11. Electrolysis reactor of the second option of the four-step Cu–Cl cycle (adapted from [22]).

bench-scale apparatus and for only individual steps, not the overall cycle, the simulation is compared with these experimental results to make sure that the trends are conformable. Finally, there are some theoretical studies about the Cu–Cl cycle in the literature that are given in the reference part of this study. To facilitate the validation of the results here, a comparison is made among the previous studies on the Cu–Cl cycle (see Table VI) and other hydrogen production processes such as steam methane reforming (SMR) and sulfur-iodine (SI) cycle.

As shown in Table VI, a conceptual process design based on the three-reaction Cu–Cl cycle has been developed to

produce 125 MT of hydrogen/day by Ferrandon *et al.* [22]. Defining efficiency as energy out divided by energy in results in estimated efficiency of around 39%. The voltage assumed for the electrolyzer is 0.7 V, which is for ambient conditions. Operating costs were also estimated using a tool called Hydrogen Analysis (H2A). The estimated cost of producing hydrogen is \$3.07/kg H₂ with a range from \$3.60 to 2.80/kg H₂ depending on the capital investment, amount of equity financing, and the cost of thermal and electrical energies. These results from Argonne National Laboratory vary in a more recent study by Lewis *et al.* [16,17]. On the basis of the earlier assumptions (used by Ferrandon *et al.* [22]), Lewis *et al.* [16,17] have estimated the cost and efficiency of hydrogen production as \$3.30/kg H₂ and 40.4%, respectively.

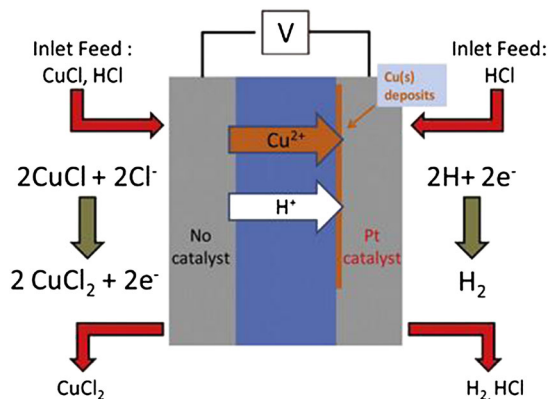


Figure 12. Schematic of electrolysis process in the second option of the four-step Cu–Cl cycle [20].

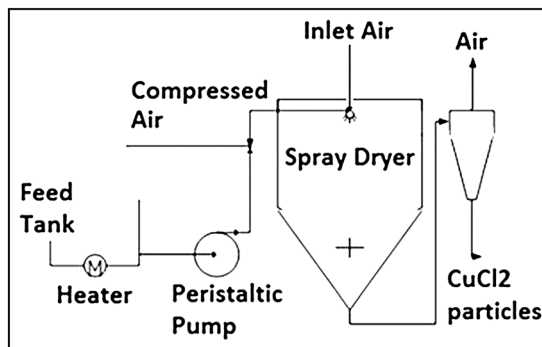


Figure 13. Spray drying of CuCl₂(aq) (adapted from [20]).

A number of sensitivity analyses were run on the economics. Depending on the sensitivity tested, the cost of hydrogen can range from \$3.00 to 3.95/kg H₂.

Besides the above-mentioned studies on the Cu–Cl cycle by Argonne National Laboratory in the US, there have been some preliminary studies at UOIT as well. For example, Orhan *et al.* [19] have performed a cost estimation for the five-step Cu–Cl cycle on the basis of energy

and exergy analyses of the cycle. The study applies the sixth-tenths-factor rule in determining the fixed capital investment and total production cost for a plant capacity of 5 t/day hydrogen on the basis of the data for a similar process (the SI cycle). In the study by Orhan *et al.* [19], the cost of producing hydrogen using the five-step thermochemical Cu–Cl cycle is \$1.68/kg H₂. The energy efficiency of the cycle was stated as 43% for this estimation.

Table V. Mass flow rates (t/h) of main streams in the simulation of the four-step Cu–Cl cycle.

Stream	Hydrolysis reactor		Oxy-decomposition		Dryer		Electrolyzer	
	Feed	Product	Feed	Product	Feed	Product	Feed	Product
H ₂ O	925	-	-	-	-	624.3	-	-
HCl	-	2.72	-	-	-	-	2.72	-
CuCl	-	-	-	411.8	-	-	-	-
CuCl(aq)	-	-	-	-	-	-	650	-
CuCl ₂	158.5	-	-	-	-	158.5	-	-
CuCl ₂ (aq)	-	-	-	-	783.1	-	-	783.1
Cu ₂ OCl ₂	-	449.1	449.1	-	-	-	-	-
O ₂	-	-	-	33.3	-	-	-	-
H ₂	-	-	-	-	-	-	-	4.2

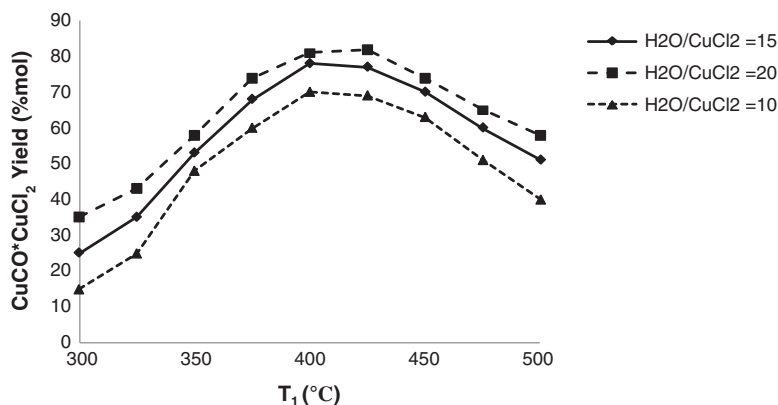


Figure 14. Variation of the CuO*CuCl₂ yield with reaction temperature.

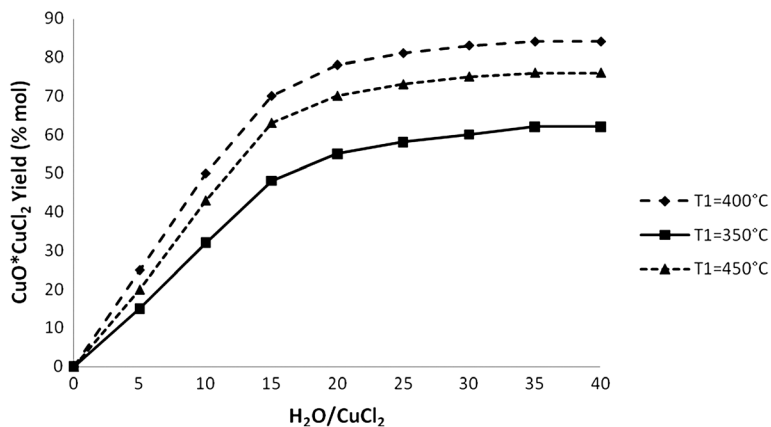


Figure 15. Variation of CuO*CuCl₂ yield with H₂O/CuCl₂ ratio.

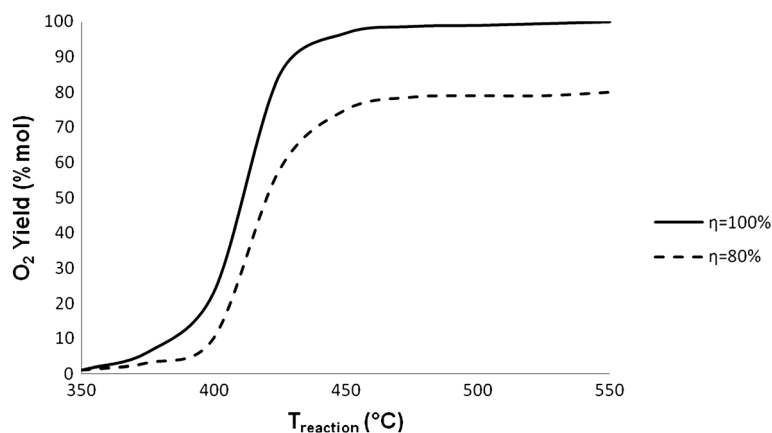


Figure 16. Variation of oxygen yield with the oxy-decomposition reaction temperature.

Table VI. Comparison of studies on the Cu–Cl cycle.

	Three-step Cu–Cl Cycle		Four-step Cu–Cl Cycle		Five-step Cu–Cl Cycle		Cost (\$/kg H ₂)	Reference
	η (%)	η_{ex} (%)	η (%)	η_{ex} (%)	η (%)	η_{ex} (%)		
Results in this study	-	-	43.8	9.8	-	-	2.80	
Argonne National Lab	40.4	-	-	-	-	-	3.30	[16, 17]
Previous theoretical studies	39	-	-	-	-	-	3.07	[22]
	-	-	-	-	43.0	7.9	1.68	[19]
	41.65	-	-	-	44.5	-	-	[23]
	-	-	43	-	-	-	1.52	[14]

Because of lack of data at that time, this analysis, however, only considered five main steps and does not include process flow sheet parameters such as heat exchanger duties, shaft work, and so on.

Chukwu [23] has reported the energy efficiency of the five-step Cu–Cl cycle as 45.5% and three-step Cu–Cl cycle as 41.65%. Also, a recent study has been carried out by Naterer *et al.* [14] estimating the cost and efficiency of the four-step Cu–Cl cycle as \$1.52/kg H₂ and 43%, respectively.

Williams *et al.* [24] have analyzed a hydrogen production using SMR technology. In the study, the cost of producing hydrogen by SMR varies between \$1.50/kg H₂ for large-scale production such as over 500 t/day and \$3.75/kg H₂ for small-scale production below 500 kg/day. In this calculation, the natural gas price of \$7.00/GJ has been assumed. In SMR technology, natural gas is used for energy source and feedstock, and thus, the cost of produced hydrogen depends on the cost of natural gas.

Hydrogen production using an SI thermochemical cycle has been studied by Brown *et al.* [25]. It has been reported that for a hydrogen production plant with a capacity of 584 t/day, the cost varies between \$1.53/kg H₂ and \$2.01/kg H₂. In the study, an energy efficiency of 42% has also been calculated.

The comparison of these previous studies on the Cu–Cl cycle and similar hydrogen production processes (SMR and SI) shows that the results in this study are valid enough to be used in the future studies. With ongoing research, the results

in this study can assist the efforts to understand the thermodynamic losses in the cycle, to improve efficiency, and reduce cost to facilitate eventual commercialization. It also indicates that the designs presented in this study for the Cu–Cl thermochemical water decomposition cycles can be good candidates for the future applications of hydrogen production.

6. CONCLUSIONS AND RECOMMENDATIONS

A design and simulation study of the four-step Cu–Cl cycle using Aspen Plus software is successfully undertaken in this paper. The design and analysis techniques presented in this study require a minimum of available data and provides effective assistance in improving and optimizing thermal systems, particularly when they are complex and/or in cases where conventional optimization techniques cannot be applied in system optimization. These analyses are useful tools in evaluating the potential for improving the cycle efficiency and cost effectiveness. This information can assist ongoing efforts to understand the thermodynamic losses in the cycle, to improve efficiency, and to facilitate eventual commercialization.

The analysis, design, and simulation reported in this study of a Cu–Cl thermochemical water decomposition cycle for hydrogen production have allowed several main conclusions to be drawn.

- It is found that the hydrolysis reactors with smaller capacity and larger (15/1 and more) steam to CuCl ratio are desirable to increase the reaction efficiency and prevent the formation of side products such as CuO and CuC. In contrast, the larger capacity oxy-decomposition reactors with longer residence time are preferable to allow enough time for the copper oxychloride time to decompose. Therefore, 10 (or more) small-scale hydrolysis reactors can feed one oxy-decomposition reactor with large capacity to keep continuity of the flow in the overall cycle.
- In an oxy-decomposition reactor, oxygen generation starts at a temperature as low as 350 °C and increases to a peak point at around 450 °C. The oxygen yield remains fairly constant with an increase in temperature above 450 °C. Traces of side products (i.e., chlorine gas) are also observed in this model analysis at incomplete reaction cases. The side-products generation increases with temperature and peaks at about 450 °C, then starts declining as the temperature of the reactor is increased. At a reactor temperature of 550 °C, the generation rate of side products is negligible. This undesirable side product can be eliminated by better reactor designs and choice of operating conditions.
- As reaction temperature increases, the reaction heat load of the oxy-decomposition step increases.
- The electrolyzer design is the most challenging step in this cycle. More rigorous and realistic unit operations and thermodynamic models should be developed to design this step to better represent the actual electrolysis process. A low-cost material for the membrane of the electrolyser should be chosen. In addition, there is a need for a good catalyst for the process and a way to reduce the energy requirement by lowering the cell potential.
- Effects of reaction kinetics are crucial in the oxygen production step. To improve the reaction efficiency and product yield, optimum kinetics should be determined, including the characteristics of the products from the fluidized bed and side reactions.
- Research into analysis and comparison of different methods of recovering heat from the molten CuCl are required to establish the best method for recovering heat from the molten salt. Future studies should aim to determine the best configuration of injectors, number of injectors, droplet diameters, and potential dust/particle in the outlet air stream.
- To thoroughly understand the heat recovery system for the cycle, a detailed pinch analysis of the heat exchangers should be undertaken to determine the best heat matching. An integrated heat exchange network should be designed to determine material, size, and number of heat exchangers and other heat management equipments.
- Detailed research on materials and equipment of heat exchangers should be carried out, and effective methods should be specified for the drying step. The ways of how to use low-temperature waste heat from nuclear reactors for the drying process should be determined.

- More experimental studies on the individual process steps are required to validate the results and better estimate the thermodynamic properties of the cycle compounds and components. In addition to small-scale semi-continuous experiments of individual steps, a closed loop experimental setup of complete cycle should be build to determine the thermal management and energy handling options within the cycle. Such a closed loop network is vital to examine heat recovery opportunities, use the heat from the process streams efficiently, and decrease the external heat demand.
- Considerations for coupling of a thermochemical hydrogen plant with a nuclear power plant must be taken into account. Most of nuclear reactors in North America are water cooled and operates at a temperature range of 300–400 °C, whereas waste heat from these reactors is at 70–80 °C. In contrast, the maximum operation temperature in the Cu–Cl cycle is around 550 °C. The heat upgrading methods should be examined to specify how to use process/waste energy from the nuclear reactor.

ACKNOWLEDGEMENT

The authors gratefully acknowledge the financial support provided by the Ontario Research Fund and Atomic Energy of Canada Limited.

REFERENCES

1. Al-Dabbagh AW, Lu L. Design and reliability assessment of control systems for a nuclear-based hydrogen production plant with copper–chlorine thermochemical cycle. *International Journal of Hydrogen Energy* 2010; **35**:966–977.
2. Daggupati VN, Naterer GF, Gabriel KS, Gravelins RJ, Wang ZL. Equilibrium conversion in Cu–Cl cycle multiphase processes of hydrogen production. *Thermochemical Acta* 2009; **496**:117–123.
3. Daggupati VN, Naterer GF, Gabriel KS. Diffusion of gaseous products through a particle surface layer in a fluidized bed reactor. *International Journal of Heat and Mass Transfer* 2010; **53**:2449–2458.
4. Daggupati VN, Naterer GF, Gabriel KS, Gravelins RJ, Wang ZL. Solid particle decomposition and hydrolysis reaction kinetics in Cu–Cl thermochemical hydrogen production. *International Journal of Hydrogen Energy* 2010; **35**:4877–4882.
5. Ferrandon MS, Lewis MA, Alvarez F, Shafirovich E. Hydrolysis of CuCl₂ in the Cu–Cl thermochemical cycle for hydrogen production: experimental studies using a spray reactor with an ultrasonic atomizer. *International Journal of Hydrogen Energy* 2010; **35**:1895–1904.

6. Ferrandon MS, Lewis MA, Tatterson DF, Doizi D, Croize L, Dauvois V, Roujou JL, Zanella Y, Gross A, Carles P. Hydrogen production by the Cu–Cl thermochemical cycle: investigation of the key step of hydrolysing CuCl_2 to Cu_2OCl_2 and HCl using a spray reactor. *International Journal of Hydrogen Energy* 2010; **35**:992–1000.
7. Jaber O, Naterer GF, Dincer I. Heat recovery from molten CuCl in the Cu–Cl cycle of hydrogen production. *International Journal of Hydrogen Energy* 2010; **35**:6140–6151.
8. Ranganathan S, Easton EB. Ceramic carbon electrode-based anodes for use in the Cu–Cl thermochemical cycle. *International Journal of Hydrogen Energy* 2010; **35**:4871–4876.
9. Ranganathan S, Easton EB. High performance ceramic carbon electrode-based anodes for use in the Cu–Cl thermochemical cycle for hydrogen production. *International Journal of Hydrogen Energy* 2010; **35**:1001–1007.
10. Wang ZL, Naterer GF, Gabriel KS, Gravelins R, Daggupati VN. Comparison of sulphur-iodine and copper–chlorine thermochemical hydrogen production cycles. *International Journal of Hydrogen Energy* 2010; **35**:4820–4830.
11. Zamfirescu C, Dincer I, Naterer GF. Thermophysical properties of copper compounds in copper–chlorine thermochemical water splitting cycles. *International Journal of Hydrogen Energy* 2010; **35**:4839–4852.
12. Zamfirescu C, Naterer GF, Dincer I. Kinetics study of the copper/hydrochloric acid reaction for thermochemical hydrogen production. *International Journal of Hydrogen Energy* 2010; **35**:4853–4860.
13. Rosen MA, Naterer GF, Chukwu CC, Sadhankar R, Suppiah S. Nuclear-based hydrogen production with a thermochemical copper–chlorine cycle and supercritical water reactor: equipment scale-up and process simulation. *International Journal of Hydrogen Energy* 2012; **36**:456–465.
14. Naterer GF, Suppiah S, Lewis M, Gabriel K, Dincer I, Rosen MA, Fowler M, Rizvi G, Easton EB, Ikeda BM, Kaye MH, Lu L, Pioro I, Spekkens P, Tremaine P, Mostaghimi J, Avsec J, Jiang J. Recent Canadian advances in nuclear-based hydrogen production and the thermochemical Cu–Cl cycle. *International Journal of Hydrogen Energy* 2009; **34**:2901–2917.
15. Wang ZL, Naterer GF, Gabriel KS. Multiphase reactor scale-up for Cu–Cl thermochemical hydrogen production. *International Journal of Hydrogen Energy* 2008; **33**:6934–6946.
16. Lewis MA, Ferrandon MS, Tatterson DF, Mathias P. Evaluation of alternative thermochemical cycles—Part III further development of the Cu–Cl cycle. *International Journal of Hydrogen Energy* 2009; **34**:4136–4145.
17. Lewis MA, Masin JG. The evaluation of alternative thermochemical cycles—part II: the down-selection process. *International Journal of Hydrogen Energy* 2009; **34**:4125–4135.
18. Naterer GF, Suppiah S, Stolberg L, Lewis M, Ferrandon M, Wang Z, Dincer I, Gabriel K, Rosen MA, Secnik E, Easton EB, Trevani L, Pioro I, Tremaine P, Lvov S, Jiang J, Rizvi G, Ikeda BM, Lu L, Kaye M, *et al.* Clean hydrogen production with the Cu–Cl cycle—progress of international consortium, I: experimental unit operations. *International Journal of Hydrogen Energy* 2011; **36**:15472–15485.
19. Orhan MF, Dincer I, Naterer GF. Cost analysis of a thermochemical Cu–Cl pilot plant for nuclear-based hydrogen production. *International Journal of Hydrogen Energy* 2008; **33**:6006–6020.
20. Naterer GF, Suppiah S, Stolberg L, Lewis M, Wang Z, Daggupati V, Gabriel K, Dincer I, Rosen MA, Spekkens P, Lvov SN, Fowler M, Tremaine P, Mostaghimi J, Easton EB, Trevani L, Rizvi G, Ikeda BM, Kaye MH, Lu L, Pioro I, Smith WR, Secnik E, Jiang J, Avsec J. Canada's program on nuclear hydrogen production and the thermochemical Cu–Cl cycle. *International Journal of Hydrogen Energy* 2010; **35**:10905–10926.
21. Orhan MF, Dincer I, Rosen MA. Exergy analysis of heat exchangers in the copper–chlorine thermochemical cycle to enhance thermal effectiveness and cycle efficiency. *International Journal of Low-Carbon Technologies* 2011; **6**:156–164.
22. Ferrandon MS, Lewis MA, Tatterson DF, Nankanic RV, Kumarc M, Wedgewood LE, Nitsche LC. The hybrid Cu–Cl thermochemical cycle. I. Conceptual process design and H2A cost analysis. II. Limiting the formation of CuCl during hydrolysis. NHA Annual Hydrogen Conference, Sacramento Convention Center, CA; March 30–April 3, 2008.
23. Chukwu C. Process analysis and aspen plus simulation of nuclear-based hydrogen production with a copper–chlorine cycle. *MASc Thesis in Mechanical Engineering, UOIT, Oshawa*, 2008.
24. Williams RB, Kornbluth K, Erickson PA, Jenkins BM, Gildart MC. Estimates of hydrogen production potential and cost from California landfill gas. 15th European Biomass Conference and Exhibition, 7–13 May 2007, Berlin, Germany.
25. Brown LC, Besenbruch GE, Lentsch RD, Schultz KR, Funk JF, Pickark PS, Marshall, AC, Showalter, SK. High efficiency generation of hydrogen fuels using nuclear power. Technical report GA-A24285 General Atomics. San Diego, CA, 2003.